Available online at www.sciencedirect.com
SCIENCE DIRECT®

ELSEVIER

Systems & Control Letters 51 (2004) 15–22

SYSTEMS & CONTROL LETTERS
www.elsevier.com/locate/sysconle

A noncausal framework for model-based feedback control of spatially developing perturbations in boundary-layer flow systems. Part II: numerical simulations using state feedback

Patricia Cathalifaud*, Thomas R. Bewley

Flow Control Lab, Department of MAE, UC San Diego, La Jolla, CA 92093-0411, USA

Received 8 April 2002; received in revised form 28 April 2003; accepted 22 May 2003

Abstract

We present numerical results illustrating the successful state feedback control of a spatially developing boundary-layer flow system. Control is applied using the noncausal framework developed in Part I of this study. After addressing some important regularization issues related to the proper treatment of the infinite-dimensional nature and semi-infinite spatial extent of the present system, we compute the state-feedback control gains according to the equations developed in Part I at several spanwise wavenumbers β. We then inverse transform the result to obtain spatial convolution kernels for determining the control feedback. The effectiveness of the controls computed using these feedback kernels, which are well resolved on the computational grid and spatially localized in the spanwise direction, is tested using direct numerical simulation of the boundary-layer flow system. A significant damping of the flow perturbation is observed, which is of the same order as the damping that arises when applying significantly more expensive iterative adjoint-based control optimization schemes.

Keywords: Flow control; Spatially localized convolution kernels; Control regularization; Boundary-layer DNS

1. Introduction

The transition of a boundary-layer flow system from the laminar state to the turbulent state is triggered via mechanisms of flow instability whose physical explanation and feedback stabilization are current areas of active fundamental and applied research. The present paper considers small, spatially developing, three-dimensional perturbations to a laminar boundary-layer flow. Such perturbations often lead to subcritical transition to turbulence. Since the system eigenfunctions in boundary-layer flows are highly nonorthogonal, analysis and control strategies based on the system eigenvalues alone are generally inadequate for this system, and linear analyses based on pseudo-modes (see [14,15]) and input/output transfer function norms (see [2,3]) are preferred. In physical terms, streamwise vortices which happen to appear upstream evolve spatially into very strong streamwise streaks downstream; these streamwise streaks are often strong enough to trigger secondary (nonlinear) instability mechanisms. The purpose of this paper is to compute feedback convolution kernels to inhibit the linear algebraic growth that can lead to the

* Corresponding author. Tel.: +1-858-5344287; fax: +1-858-8223107.

E-mail addresses: catalifo@turbulence.ucsd.edu (P. Cathalifaud), bewley@ucsd.edu (T.R. Bewley).

0167-6911/04/$ - see front matter
doi:10.1016/S0167-6911(03)00183-X

triggering of such instability mechanisms via state-feedback control. The estimator developed in Part I is currently under numerical investigation and will be reported in future work.

In Part I of this work (see [4]), we introduced a new noncausal framework for feedback control of the present system which leverages the peculiar parabolic-in-space nature of boundary-layer flow systems. The reader is referred to Part I for the derivation of the control technique to be used in the present paper and discussion of how it fits in to the existing body of literature in the field of flow control.

Moving from the theoretical formulation of an appropriate control strategy for a fluid system to numerical implementation and testing such strategy is often nontrivial due to some special considerations that are required to handle properly the infinite-dimensional nature and infinite or semi-infinite spatial extent of fluid systems. The problem essentially boils down to getting the control feedback gains for the PDE system to roll off sufficiently rapidly as a function of the spatial wavenumbers, and is akin to the issue (which controls engineers are already familiar with) of getting the control feedback to roll off sufficiently rapidly as a function of the temporal wavenumber in ODE systems, as evidenced in a Bode plot. Significant progress has already been made on this subtle issue, which is discussed further in [13] for iterative adjoint-based control optimization problems and in [7] for Riccati-based feedback control calculations. After a brief discussion of the numerical discretization used in the present work in Section 2, we will discuss the important issue of regularization of the present analysis in Section 3. The resulting localized kernels are presented in Section 4, and the effectiveness of the approach is verified by the simulation results presented in Section 5.

2. Numerical discretization

The numerical discretization of the boundary-layer flow system studied in the present work (and discussed in detail in Part I) is fairly standard. In the wall-normal direction y, the actual flow perturbations evolve in a semi-infinite domain $[0, \infty]$. Numerically, we must solve the system on the finite domain $[0, y_\infty]$. The y-discretization points used in the present study are the modified Chebyshev–Gauss–Lobatto points (see [17])

$$y(i) = \frac{y_\infty}{2}\, c\, \frac{1 + \cos(\pi i/N)}{1 + c - \cos(\pi i/N)} \tag{1}$$

for $i = 1, \dots, N_y$, and appropriate boundary conditions are applied at y_∞ to emulate the far field. The normal derivative operators, $D^k = \delta^k/\delta y^k$, are approximated via a spectral collocation method, which is discussed in detail in [17]. We take special care to avoid the spurious eigenvalues discussed in [3] by using the method described by Huang and Sloan [8]. The key of this approach is the use of a polynomial of degree $(N-2)$ for the approximation of the second-order derivative term in the Orr–Sommerfeld/Squire equations when all other terms in these equations are approximated by polynomials of degree N.

We use a uniform grid in the streamwise direction x, and discretize our system using the “delta” formulation described by Middleton and Goodwin [11]. The matrix $\Omega_k = (1/\Delta) \int_0^\Delta \exp(A_k \tau)\, \mathrm{d}\tau$ that arises in this discrete-in-x problem formulation (see Part I) contains a matrix exponential, which is computed using a scaling and squaring method on Padé approximations. The details of this method may be found in [12,16].

In the spatially homogeneous spanwise direction z, the control problem is first decoupled and solved on a wavenumber-by-wavenumber basis using a Fourier representation, as discussed in Part I. We then inverse Fourier transform the resulting feedback gains to determine spatially localized feedback convolution kernels using the FFTW library presented in [6].

3. Regularization of the control

As shown in Part I, the discretized state equation may be written as

$$\delta \mathbf{q}_k = \Omega_k A_k \mathbf{q}_k + \Omega_k B_k \phi_k + \Omega_k D_k \mathbf{w}_k. \tag{2}$$

In order to insure that the control distribution varies smoothly in x, we penalize the square of $\mathrm{d}\phi/\mathrm{d}x = \mathrm{d}^2 v_w/\mathrm{d}x^2$ in the cost function

$$\mathscr{J} = \int_{x_0}^{L} \left[\int_0^\infty (\ell_v^2 v^* v + \ell_\eta^2 \eta^* \eta)\, \mathrm{d}y + \ell_{v_w}^2 v_w^* v_w + \ell_\phi^2 \phi^* \phi + \ell_s^2 \frac{\partial \phi^*}{\partial x} \frac{\partial \phi}{\partial x} \right] \mathrm{d}x,$$

which may be approximated, after discretizing in x and y, by

$$\mathscr{J} = \sum_{i=0}^{N} \Delta[(\mathbf{q})_i^* Q \mathbf{q}_i + \ell_\phi^2 \phi_i^* \phi_i] + \sum_{i=1}^{N} \Delta \left[\ell_s^2 \frac{\partial \phi_i^*}{\partial x} \frac{\partial \phi_i}{\partial x} \right], \tag{3}$$

where

$$Q = \begin{pmatrix} \ell_v^2 I_s & 0 & 0 \\ 0 & \ell_\eta^2 I_s & 0 \\ 0 & 0 & \ell_{v_w}^2 \end{pmatrix},$$

and I_s is a diagonal matrix with the corresponding local wall-normal grid spacing on the elements of the diagonal. Note that $\partial\phi_i/\partial x$ may be approximated by $(\phi_i - \phi_{i-1})/\Delta$. By defining $\phi_{-1} = \phi_0$ we can therefore write the cost function as

$$\mathscr{J} = \sum_{i=0}^{N} \left[\Delta \mathbf{q}_i^* Q \mathbf{q}_i + \left(\Delta \ell_\phi^2 + \frac{\ell_s^2}{\Delta} \right) \phi_i^* \phi_i + \frac{\ell_s^2}{\Delta} \phi_{i-1}^* \phi_{i-1} \right] - 2 \frac{\ell_s^2}{\Delta} \phi_0^* \phi_0 - \sum_{i=1}^{N} \left[\frac{\ell_s^2}{\Delta} (\phi_{i-1}^* \phi_i + \phi_i^* \phi_{i-1}) \right].$$

In order to express this cost function in the classical quadratic form, we append ϕ_{k-1} to our state vector. We thus define

$$\mathbf{q}_k^r = \begin{pmatrix} \mathbf{q}_k \\ \phi_{k-1} \end{pmatrix}. \tag{4}$$

Noting that $\delta\phi_{k-1} = (1/\Delta)\phi_k - (1/\Delta)\phi_{k-1}$, and using the discrete state-space evolution of state (2), we obtain a new discretized state equation

$$\delta \mathbf{q}_k^r = A_k^r \mathbf{q}_k^r + B_k^r \phi_k + D_k^r \mathbf{w}_k, \tag{5}$$

where

$$A_k^r = \begin{pmatrix} \Omega_k A_k & 0 \\ 0 & -1/\Delta \end{pmatrix}, \quad D_k^r = \begin{pmatrix} \Omega_k D_k \\ 0 \end{pmatrix},$$

$$B_k^r = \begin{pmatrix} \Omega_k B_k \\ 1/\Delta \end{pmatrix}.$$

Note that (5) and (2) are completely equivalent. Now define the augmented state

$$\mathbf{q}_k^{\mathrm{a}} = \begin{pmatrix} \mathbf{q}_k^r \\ \mathbf{q}_k^{\mathbf{w}} \end{pmatrix}, \tag{6}$$

where $\mathbf{q}_k^{\mathbf{w}}$ follows the disturbance model defined in Part I. Using this augmented state $\mathbf{q}_k^{\mathrm{a}}$ in the cost function, we obtain

$$\mathscr{J} = \sum_{i=0}^{N} [(\mathbf{q}^{\mathrm{a}})_i^* Q^{\mathrm{a}} \mathbf{q}_i^{\mathrm{a}} + \phi_i^* R \phi_i + (N\mathbf{q}_i^{\mathrm{a}})^* \phi_i + \phi_i^* N \mathbf{q}_i^{\mathrm{a}}], \tag{7}$$

where

$$Q^{\mathrm{a}} = \begin{pmatrix} Q^r & 0 \\ 0 & 0 \end{pmatrix}, \quad Q^r = \begin{pmatrix} \Delta Q & 0 \\ 0 & \ell_s^2/\Delta \end{pmatrix},$$

$$R = \Delta \ell_\phi^2 + \ell_s^2/\Delta \quad \text{and} \quad N = (0 \ \ -\ell_s^2/\Delta \ \ 0).$$

Now define a new control variable

$$\phi_i^N = R^{-1/2} N \mathbf{q}_i^{\mathrm{a}} + R^{1/2} \phi_i = -(\ell_s^2/\Delta) R^{-1/2} \phi_{i-1} + R^{1/2} \phi_i. \tag{8}$$

Using relations (7) and (8), the cost function becomes a standard discrete quadratic form

$$\mathscr{J} = \sum_{i=0}^{N} [(\mathbf{q}^{\mathrm{a}})_i^* Q^N \mathbf{q}_i^{\mathrm{a}} + \phi_i^{N^*} \phi_i^N], \tag{9}$$

where $Q^N = Q^{\mathrm{a}} - N^* R^{-1} N$, and plant (2) is transformed to the standard discrete state space form

$$\delta \mathbf{q}_k^{\mathrm{a}} = A_k^N \mathbf{q}_k^{\mathrm{a}} + B_k^N \phi_k^N, \tag{10}$$

where $A_k^N = A_k^A - B_k^A R^{-1} N$ and $B_k^N = B_k^A R^{-1/2}$.

We can now find a feedback control law for this problem as described in Part I:

$$\phi_k^N = -K_{k+1}^N \mathbf{q}_k^{\mathrm{a}}. \tag{11}$$

Combining (11), (10) and (8) we can express ϕ_k as a simple function of $\mathbf{q}_0^{\mathrm{a}}$:

$$\phi_k = K_{k+1}^0 \mathbf{q}_0^{\mathrm{a}}, \tag{12}$$

where $K_{k+1}^0 = -R^{-1/2}(K_{k+1}^N + R^{-1/2}N) \prod_{i=0}^{k-1} [A_i^{\mathrm{a}} - R^{-1/2}(K_{i+1}^N + R^{-1/2}N) B_i^{\mathrm{a}}]$.

Our objective is to find a sufficiently smooth control that minimizes the perturbation energy $\sum_{i=0}^{N} \Delta(\mathbf{q})_i^* Q \mathbf{q}_i$. When the spanwise wavenumber β tends to zero, we find that the gain matrix K^0 for the control problem as formulated

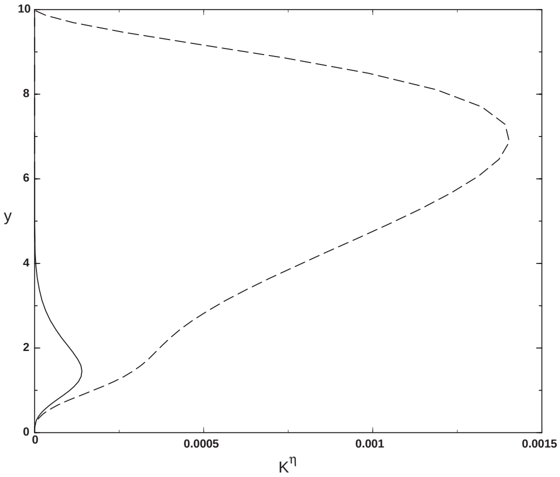

Fig. 1. Control gain for β=0.1 related to the normal vorticity, at the middle of the control domain [0.5, 0.8], using (—) a wall-weighted objective function, and (- - -) an objective function without a wall-weighting term.

thus far is large for $y > \delta_x$, as depicted in the dashed curve in Fig. 1. This means that flow perturbations outside the boundary layer affect the control at the wall strongly, which is not intended. Further, since the boundary-layer flow actually takes place in a semi-infinite domain, $0 \leqslant y < \infty$, K^0 depends strongly on the numerical upper bound y_∞ when β goes to zero, which is nonphysical.

We must therefore reformulate our control objective in order to arrive at a physically meaningful control strategy. Note that we are not actually interested in controlling the free-stream perturbations. Furthermore, since $\mathbf{q}_0^a$ will ultimately be estimated by measurements taken at the wall, we will probably have only a poor estimate of the flow perturbations outside the boundary layer in the final (estimator-based) implementation. We thus refine our objective function such that the control minimizes the energy of the perturbation only *inside* the boundary layer. To do so, we simply use the second wall-normal derivative of the longitudinal velocity of the base flow, $\delta^2 U/\delta y^2$ (hereafter denoted by U''), to weight appropriately the diagonal matrix I_s in Q, where $(I_s)_{ij} = \delta_{ij}(y_{i+1} - y_i)$ $|U_i''/U_{\max}''|$. Fig. 1 represents the profiles of the control gain for a wavenumber of $\beta = 0.1$, before and after weighting the matrix I_s with $|U''/U_{\max}''|$. We see that, in the weighted control problem, the resulting control feedback is no longer as heavily dependent on the perturbations outside the boundary layer.

4. Spatially localized convolution kernels

By inverse Fourier transforming the gain matrices K^0, we obtain feedback convolution kernels which are spatially localized in the spanwise direction z (see [1,7]). Physically, this means that the control at a spanwise location z depends only on the input perturbation in the vicinity of this spanwise location. Fig. 2 depicts representative convolution kernels relating the streamwise and wall-normal velocity of perturbation at $x_0 = 0.5$ to the control input on the wall on $x \in [0.5, 0.8]$ as a result of the present control formulation. To obtain the control at the wall position x_k and z, we simply convolve the kernel in the plane at the streamwise location x_k with the input perturbation $\mathbf{q}_0^a$ in the vicinity of the spanwise location z, as depicted in Fig. 3. As expected, the convolution kernels depicted in Fig. 2 do not exhibit spatial localization in the streamwise direction x, but are elongated in this direction.

It is significant to note that our objective function, which up to this point has been targetted on the minimization of the perturbation energy over the entire streamwise extent $[x_0, x_N]$ of the domain of control under consideration, may easily be generalized using present formulation to target specifically the perturbation energy at the end of the control domain, x_N. To accomplish this, we simply add to the cost function (3) a penalty term on the energy of the perturbation at the end of the control domain

$$\mathscr{J} = \sum_{i=0}^{N} \Delta[(\mathbf{q})_i^* Q \mathbf{q}_i + \ell_\phi^2\, \phi_i^* \phi_i] + \sum_{i=1}^{N} \Delta\left[\ell_s^2\, \frac{\partial \phi_i^*}{\partial x}\, \frac{\partial \phi_i}{\partial x}\right] + \ell_N (\mathbf{q})_N^* \Sigma_N^{11} \mathbf{q}_N, \qquad (13)$$

where Σ_N^{11} is the initial condition of the Riccati equation which arises when solving the feedback control problem (see Part I). We may target these outflow (“terminal”) perturbations exclusively simply by setting $Q = 0$. Fig. 4 represents the streamwise and wall-normal kernels for this new optimization problem.

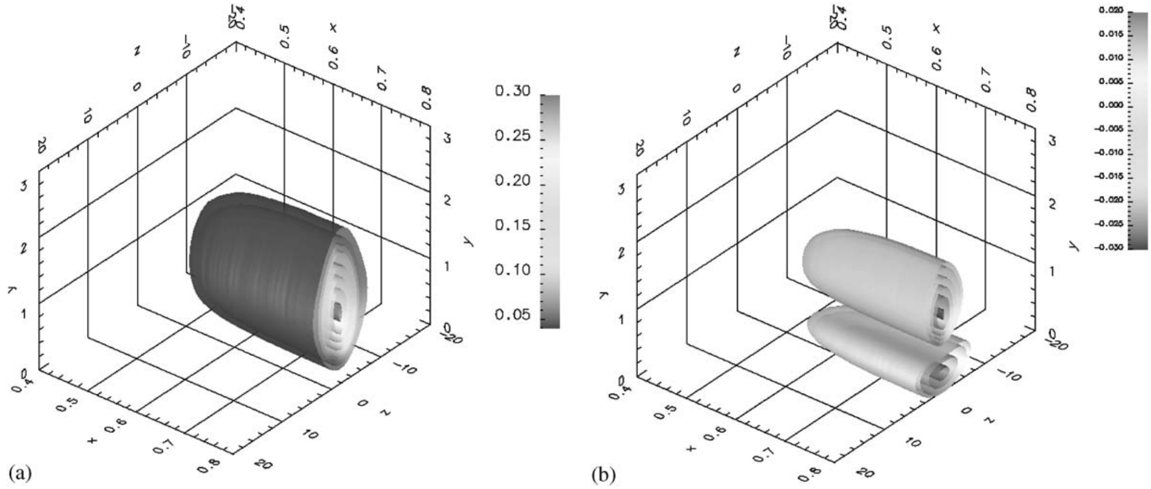

Fig. 2. Isosurfaces of the components of the feedback convolution kernel $K^0(x, y, z)$ relating (a) the streamwise component of the velocity u $(x = 0.5, y, z)$ and (b) the wall-normal component of the velocity v $(x = 0.5, y, z)$ to the control input ϕ $(x, z = 0)$ on $x \in [0.5, 0.8]$. The cost function in this case is the minimization of the perturbation energy on the interval $x \in [0.5, 0.8]$.

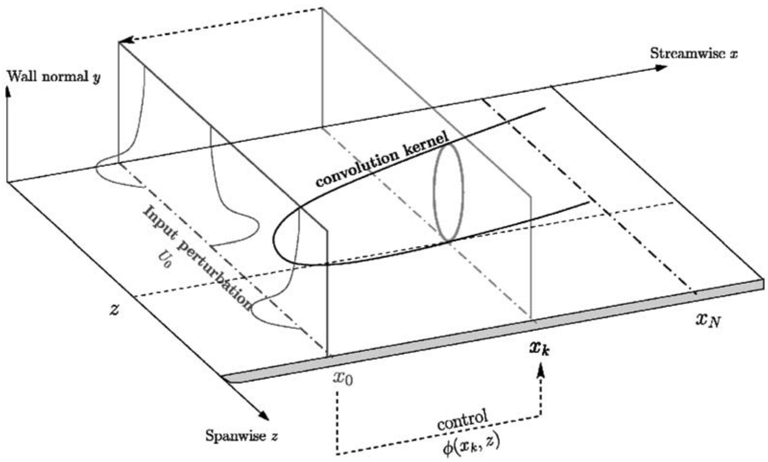

Fig. 3. Relation between the flow system and the control input. The control ϕ $(x = x_k, z)$ is found by convolving the feedback kernel K^0 in the plane $x = x_k$ with the augmented state $\mathbf{q}_0^{\mathrm{a}}$ in the vicinity of the spanwise location z.

5. Numerical simulations

By inserting the feedback convolution kernels illustrated in Fig. 2 into a direct numerical simulation (DNS) code, we now perform simulations of the feedback controlled system, assuming full knowledge of the initial perturbation $\mathbf{q}_0^{\mathrm{a}}$. For comparison, we have also calculated the effectiveness of controls determined by applying an iterative, adjoint–based control optimization strategy, as developed by Cathalifaud and Luchini [5].

To perform the boundary-layer flow simulations, we used the spectral DNS code developed by Lundbladh et al. [10], which accurately solves the full nonlinear 3D incompressible Navier–Stokes equations in the boundary layer and correctly accounts for the

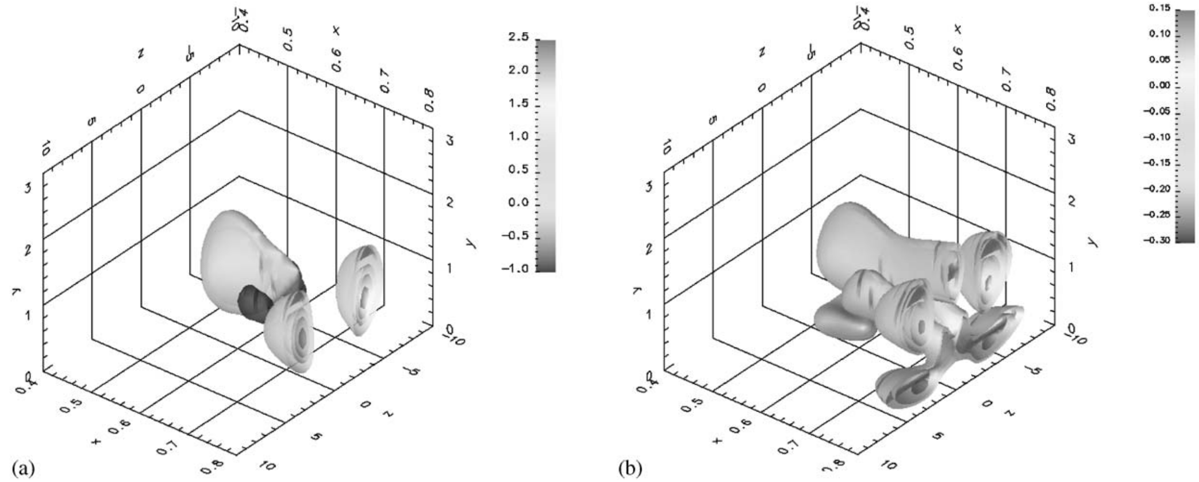

Fig. 4. Isosurfaces of the components of the feedback convolution kernels $K^0(x,y,z)$ relating (a) the streamwise component of the velocity u $(x=0.5,y,z)$ and (b) the wall-normal component of the velocity v $(x=0.5,y,z)$ to the control input ϕ $(x,z=0)$ on $x\in[0.5,0.8]$. The cost function in this case is the minimization of the perturbation energy at $x=0.8$.

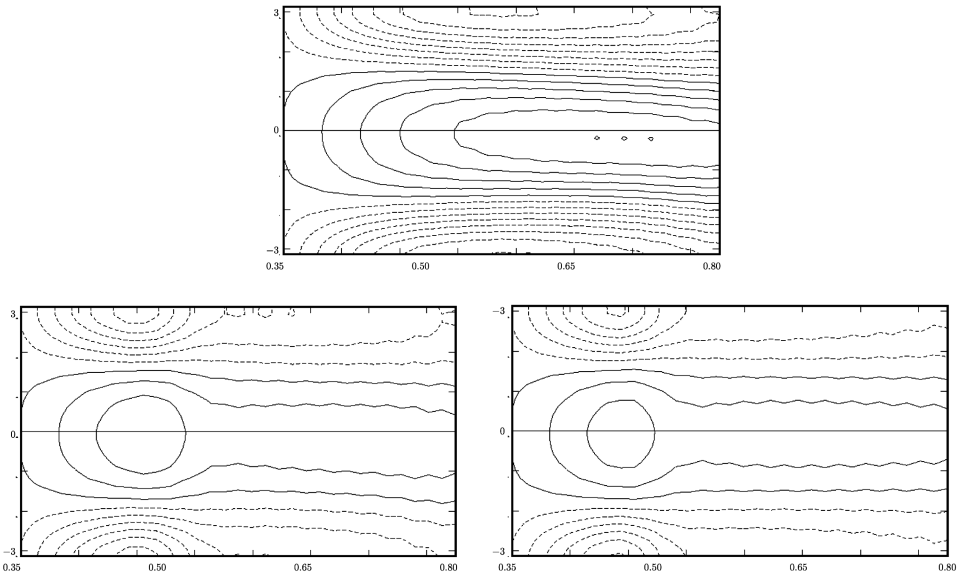

Fig. 5. Longitudinal streaks without control (top), with present feedback control strategy (bottom left), and with the iterative adjoint-based control optimisation strategy of [5] (bottom right).

effects of control inputs on the wall, as thoroughly benchmarked in [10].

Fig. 5 displays the isolines of the streamwise velocity of perturbation in a x,z plane located at $y=2.022$, both without and with control. We have tested a worst-case (a.k.a., "optimal") initial perturbation, that is, a perturbation whose energy is amplified maximally over the computational domain under consideration in the uncontrolled system. This kind of perturbation has been computed previously by Luchini [9], who found that such perturbations come in the form of stationary streamwise vortices,

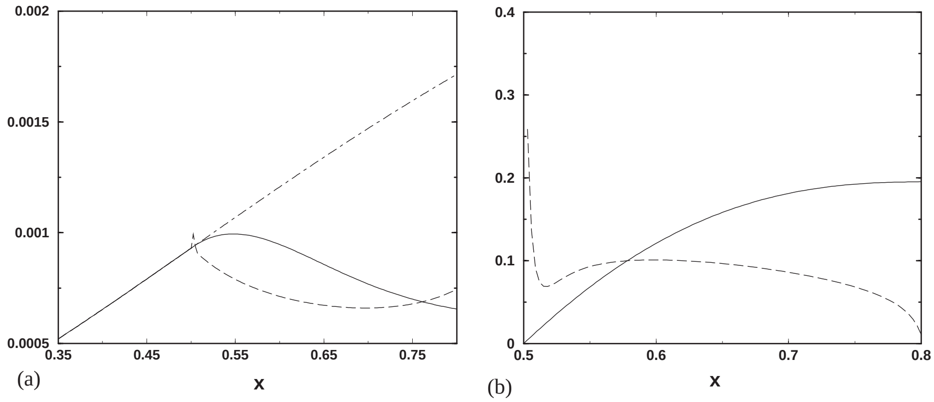

Fig. 6. (a) Evolution of the energy of perturbation E using (– · –) no control, (—) the present feedback control strategy, and (– –) the iterative adjoint-based control optimization strategy of [5]. (b) Evolution of the control energy using (—) the present strategy, and (– –) the adjoint-based strategy.

whereas the velocity field they induce is dominated by streamwise streaks. This is a typical behaviour in shear-driven flows.

The control is applied over $[x_0, x_N] = [0.5, 0.8]$, and we notice a very similar reduction of the perturbation magnitude in both the present feedback control formulation and the iterative adjoint-based control optimization.

We have also computed the energy of the perturbation $E = \int_0^\infty \int_{z_l}^{z_r} u^2 \, dz \, dy$. Fig. 6(a) displays the streamwise evolution of this energy. In the present feedback control formulation, the blowing/suction velocity v_w is part of the state vector $\mathbf{q}^a$. This means that, using the control law (12), the control at each streamwise station x_k depends on the velocity of blowing/suction at x_0, $v_w(x_0)$, which we impose to be zero; this leads to the control in the present formulation gently ramping up from zero at $x = x_0$. On the contrary, in the adjoint-based scheme the control $v_w(x_0)$ experiences a large jump at $x = x_0$, as shown in Fig. 6(b). This explains, at least in part, the difference of effect between the two control strategies. In other respects, the damping of the perturbation energy is found to be of similar order in the two cases.

6. Conclusions

Our present approach to the control of boundary-layer flow systems is a decentralized-in-z feedback strategy that takes into account the parabolic-in-x nature of boundary-layer flow systems. Using the formulation developed in Part I, we obtained well-resolved convolution control kernels that are elongated in the streamwise direction and localized in the spanwise direction. By applying these feedback kernels in a direct numerical simulation, we have shown that the resulting control is quite effective, and that it provides a damping of the perturbation energy of the same order as that obtained with much more cumbersome, iterative adjoint-based control optimization schemes.

References

[1] B. Bamieh, F. Paganini, M. Dahleh, Distributed control of spatially invariant systems, IEEE Trans. Automat. Control 47 (7) (2002) 1091–1107.
[2] T.R. Bewley, Flow control: new challenges for a new Renaissance, Prog. Aerospace Sci. 37 (2001) 21–58.
[3] T.R. Bewley, S. Liu, Optimal and robust control and estimation of linear paths to transition, J. Fluid Mech. 365 (1998) 305–349.
[4] P. Cathalifaud, T.R. Bewley, A noncausal framework for model-based feedback control of spatially-developing perturbations in boundary-layer flow systems. Part I: formulation, Systems Control Lett. 51 (2004) 1–13, this issue.
[5] P. Cathalifaud, P. Luchini, Algebraic growth in boundary layers: optimal control by blowing and suction at the wall, European J. Mech. B—Fluid 19 (2000) 469–490.
[6] M. Frigo, S.C. Johnson, The fastest Fourier transform in the west, MIT-LCS-TR-728, 1997.
[7] M. Högberg, T.R. Bewley, D.S. Henningson, Linear feedback control and estimation of transition in plane channel flow, J. Fluid Mech. 481 (2003) 149–175.

[8] W. Huang, D.M. Sloan, The pseudo-spectral method for solving differential eigenvalue problems, J. Comput. Phys. 111 (1993) 399–409.

[9] P. Luchini, Reynolds-number-independent instability of the boundary layer over a flat surface: optimal perturbations, J. Fluid Mech. 404 (2000) 289–309.

[10] A. Lundbladh, D.S. Henningson, A.V. Johansson, An efficient spectral integration method for the solution of the Navier–Stokes equations, Report No. FFA-TN 1992-28, Aeronautical Research Institute of Sweden, Bromma, 1992.

[11] R.H. Middleton, G.C. Goodwin, Digital Control and Estimation, Prentice-Hall, Englewood Cliffs, NJ, 1990.

[12] C. Moler, C. Van Loan, 19 dubious ways to compute the exponential of a matrix, SIAM Rev. 20 (1978) 4.

[13] B. Protas, T.R. Bewley, G. Hagen, A comprehensive framework for the regularization of adjoint analysis in multiscale PDE systems, J. Comput. Phys., submitted.

[14] L.N. Trefethen, A.E. Trefethen, S.C. Reddy, T.A. Driscoll, Hydrodynamic stability without eigenvalues, Science 261 (1993) 578–584.

[15] L.N. Trefethen, A.E. Trefethen, S.C. Reddy, T.A. Driscoll, Hydrodynamic stability without eigenvalues, Science 261 (1993) 578–584.

[16] R.C. Ward, Numerical computation of the matrix exponential with accuracy estimate, SIAM J. Numer. Anal. 14 (4) (1977) 600–610.

[17] J.A.C. Weidman, S.C. Reddy, A MATLAB differentiation matrix suite, 1998.